ISSN 2347 - 3983
Volume 10. No.1, January 2022
International Journal of Emerging Trends in Engineering Research
Available Online at http://www.warse.org/IJETER/static/pdf/file/ijeter011012022.pdf
https://doi.org/10.30534/ijeter/2022/011012022

Hardness and Microstructure Homogeneity of Pure Copper and Iron-Chromium Alloy Processed by Severe Plastic Deformation

Muhammad Rifai[1], Mujamilah[1], Hiroyuki Miyamoto[2]
[1]Center for Research and Technology of Nuclear Advanced Material, National Research and Innovation Agency, Serpong, Tangerang Selatan, Banten, Indonesia
[2]Department Science and Engineering, Doshisha University, Kyotanabe Campus, Kyoto, Japan

Received Date December 03, 2021 Accepted Date : December 29, 2021 Published Date : January 07, 2022

ABSTRACT

Hardness and microstructure homogeneity of pure copper and iron-chromium alloy processed by severe plastic deformation (SPD) were investigated in grain refinement. Equal channel angular pressing (ECAP) is one of the well-known techniques of the SPD technique due to their up-scale ability and other methods. SPD was applied to pure copper and iron-chromium alloy at comparable temperatures up to four passes. The microstructure and microhardness were observed and measured in the transverse plane for each billet. The homogeneity observation was carried out from the sub-surface until in the middle of the billet. The result showed that the deformed structure appeared adequately after the first pass and had a higher hardness level. The first pass showed a higher inhomogeneity factor than the fourth pass due to the homogeneity microstructure. The hardness also showed homogeneous value along the transverse plane, and it was concluded that ECAP could achieve complete homogeneity in grain refinement.

Key words : SPD; ECAP; recovery; recrystallization.

1. INTRODUCTION

Severe plastic deformation (SPD) is a well-known technique to promote the ultrafine-grained structure in metallic material without changing the sample dimension [1-5]. Equal channel angular pressing (ECAP) is one of the SPD techniques, which is the easiest to scale up among the other SPD techniques due to the similar size of the die channel with a specific angle [6-11]. Previous work showed better corrosion resistance and higher strength on metallic material in biomaterial application, especially iron-chromium alloy and copper [12-16].

The ECAP process has a high advantage on the continuous process of producing the UFG structure, which could be easier to apply in the industry. The other techniques of the SPD process are pretty challenging to scale up and use in the industry due to high energy and cost, such as the rolling and extrusion processes [5]. Microhardness measurements have been significant in investigating the homogeneity of ECAP processed material on copper [17-20] and stainless steel [21-25]. The hardness and microstructure homogeneity can be observed and evaluated on the ECAP billet sectioned with imposed strain on the material [20].

Previous research has shown that the microhardness distribution has been measured on preferred planes during the ECAP process with many microhardness indenter numbers [26-29]. The measurement has been done on the cross-sectional plane of the ECAP processed sample and analysed in terms of homogeneity and imposed strain [26-29]. These results have not provided the information on the homogeneity factor on the transverse plane, which is the most deformed one compared to other planes during the ECAP process. The transverse plane results on microhardness distribution may give important information for continuous processing for sheet metallic materials. Hardness measurements on pure copper have been measured on each longitudinal plane, which have exhibited the lower hardness on the edge of billets. Another hardness measurement has been done on the longitudinal plane, with no meaningful information of evolution hardness during the ECAP process [3,4]. This research novelty is to investigate the hardness and microstructure homogeneity of copper and iron-chromium alloy which are subjected by ECAP process and analyse it in term of grain boundary state.

In this study, the transverse plane was observed and measured due to the continuous process of ECAP techniques. The cross-sectional planes at the transverse plane of the ECAP billet could be appropriately monitored by sectioning the part of the sample billet. The previous result showed that the hardness homogeneity of metallic material by the ECAP process has a lower value on the sub-surface at the longitudinal plane [28,29]. The other research also lacks

knowledge of the effect of imposed strain along the transverse plane, especially during high-pressure torsion and ECAP processes. This research aims to investigate the hardness and microstructure homogeneity of iron-chromium alloy as face-centered cubic (FCC) and pure copper as body-centered cubic (BCC) in terms of strain energy and grain refinement along transverse planes as results of ECAP processes.

2. EXPERIMENTAL PROCEDURE

Iron chromium alloy (Cr 20%, C and N < 5ppm, Fe balanced) and pure copper (99.99%) billets were used for the ECAP process. The materials were selected due to the crystal structure of those materials. The iron-chromium alloy was processed at 423 K and pure copper at room temperature. The process temperature was decided based on the melting temperature of those materials. The billets were processed using a die channel at an angle of 90° and an intersection of 0°. It means the imposed strain is equal to one equivalent strain. Route Bc was used to carry out the ECAP process by rotating the billet by 90° in the same direction. This route was selected due to the highest deformation level and could promote the equiaxed grain, high grain misorientation, and grain refinement [13-16]. The billet of ECAP processed was cut from the plate of the transverse plane. Microhardness measurements were carried out on the transverse plane of the material, which was previously ground and polished by mechanical technique. The microhardness was carried out by Shimadzu Microhardness test from the middle into the sub-surface. The scheme of measurement can be seen in Figure 1. The microstructure was observed by scanning electron microscope (SEM) JEOL 7001F equipped with electron backscattered diffraction (EBSD), and transmission electron microscope (TEM) 2001F.

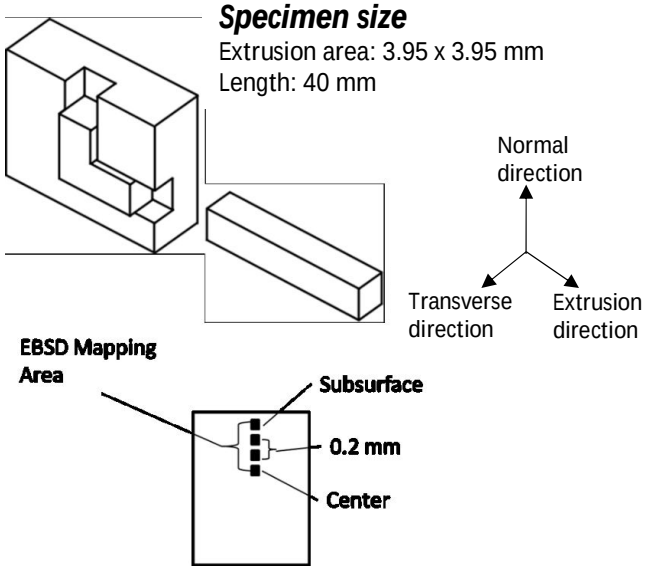

Figure 1. Scheme of ECAP process on the hardness value measurement and microstructure observation on the transverse plane.

3. RESULT

Figure 2 (a) shows the grain boundary misorientation of one pass ECAP process on pure copper by EBSD analysis. The green and pink colors refer to low angle grain boundary (LAGB) in the range $2° \leq \theta < 15°$, and high angle grain boundary (HAGB) in the range $15° \leq \theta$, respectively. The figure represents the condition of grain boundary misorientation from the middle to the subsurface, which is every 200 μm distance for every observation site. The observation was carried out on the transverse plane. The shear deformation on the sample was seen clearly in the middle of the billet (0.5 D/Do).

After one pass ECAP process, the microstructure revealed lamellar grain boundary structures along the transverse plane of the billet with 26.6° inclination due to shear deformation in Figure 2 and 3. The fraction of HAGB increased by increasing the number of ECAP passes, which correlated to previous work on copper. Lamellar boundary structure, homogeneous microstructure, and more equiaxed grain was achieved after four passes of the ECAP process, as seen in Figure 2 (b). The mean grain boundary spacing decreased by increasing the ECAP process. The value of inhomogeneity on hardness and microstructure was measured by the aspect ratio from the middle to sub-surface with a more equiaxed grain appearance. The morphology of pure copper after four ECAP processes showed UFG structure in the lamellar boundary structure.

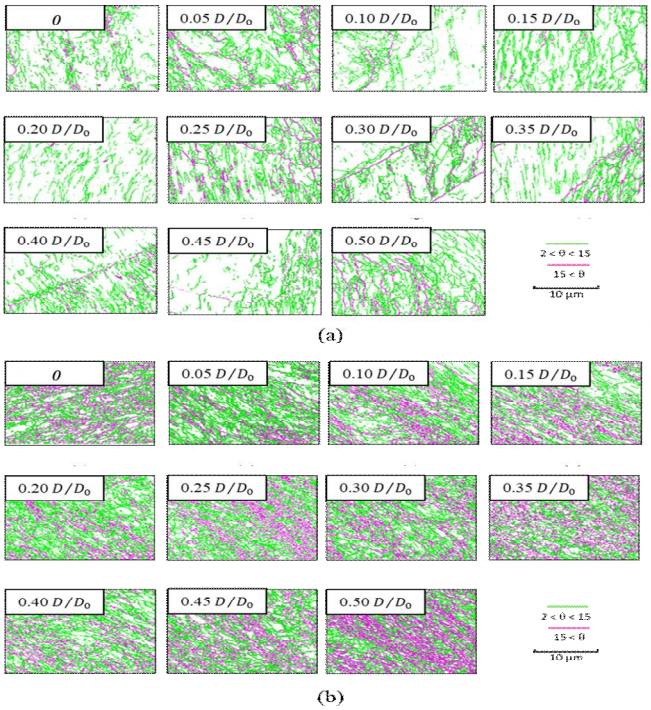

Figure 2. Misorientation image map of ECAP process on copper from the middle until sub-surface for (a) one pass and (b) four passes. The high angle grain boundary can be appeared due to initial shear deformation at one pass and the fully grain refinement can be achieved at four passes of ECAP.

The grain boundary spacing of HAGB was finer and straighter after four passes of ECAP in iron-chromium alloy, as seen in Figure 3. The microstructure also showed more equiaxed grain and homogeneous system in the middle of the billet due to shear deformation. The UFG structure in pure copper was quite coarser than iron-chromium alloy due to the energy of stacking fault and the slip plane of the material [12]. The pure copper and iron-chromium alloy have a different crystal structure and slip plane. This difference affects recovery and recrystallization behavior on the copper due to crystal structure. It was concluded that FCC material showed more equiaxed grain and homogeneous system in the middle of the billet.

Figure 4 shows the fraction of LAGB and HAGB on pure copper, and iron-chromium alloy for one and four ECAP passes. The LAGB and HAGB fractions were measured at the sample section position from the middle to the subsurface, normalized by D/Do. Both materials showed a higher fraction of HAGB in the middle due to the shear deformation at the position. The structure at the sub-surface is quite different at other locations due to deformation by the ECAP process. However, the fraction of HAGB is around 50% in the iron-chromium alloy and 45% in pure copper after four ECAP pass. This result concluded that the distribution of the HAGB fraction was homogeneous at all positions after four passes of ECAP.

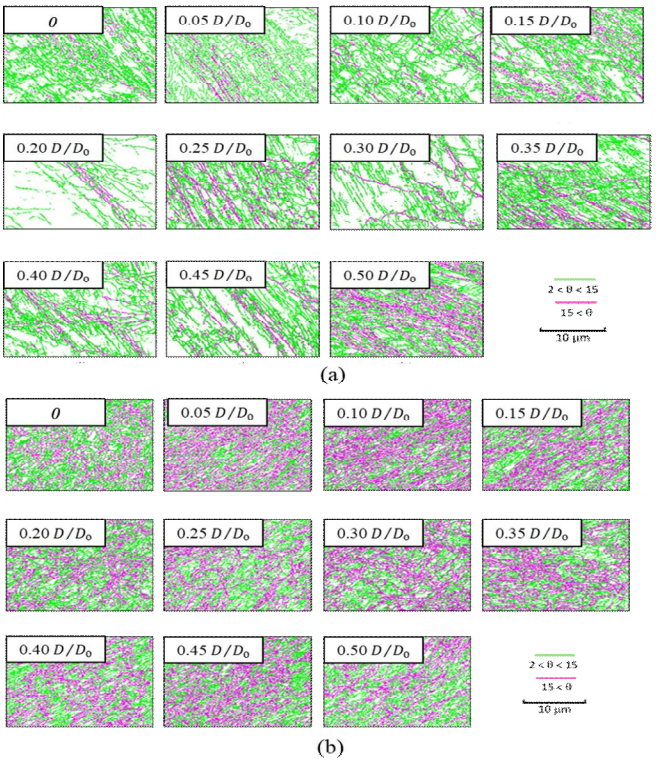

Figure 3. Misorientation image map of ECAP process on iron-chromium alloy from the middle until sub-surface for (a) one pass and (b) four passes. Low angle grain boundary can be exhibited efficiently compared to pure copper and The grain refinement can be achieved faster than pure copper.

Figure 5 shows the mean orientation of the LAGB and HAGB on pure copper, and iron-chromium alloy for one and four ECAP passes. The measurement was carried by the normalized positions, D/Do. The mean orientation data showed similar behavior with fraction value, of which the stable value was reached after four ECAP passes due to homogeneous value. The peak misorientation was reached at 23° for pure copper and 22° for iron-chromium alloy at four ECAP passes; however, the iron-chromium alloy was more stable than pure copper in mean orientation distribution. The mean orientation measurement was carried out in the LAGB and HAGB, which corresponded to recrystallized structure of the material. The ECAP processed sample showed unique characteristic on the mechanical and electrochemical behaviour due to the evolution of the grain and grain boundary structure during deformation process. This characteristic refers to the LAGB fraction, especially at pure copper due to room temperature ECAP process, of which the pure copper is harder to get recovered. The mean misorientation distribution of pure copper is higher than that of iron-chromium alloy, as seen in Figure 4. This distribution may relate to the stacking fault energy of the material [12]. The iron-chromium alloy does not show a steep peak at misorientation distribution due to the high-temperature process, annihilating dislocation, and LAGB.

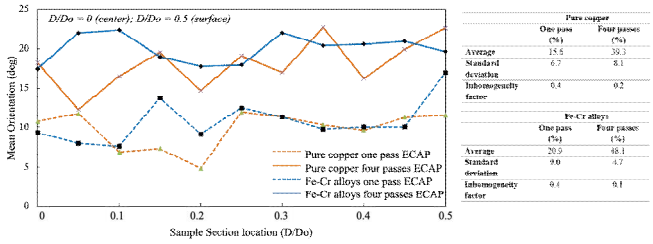

Figure 4. High angle grain boundary fraction on first and fourth ECAP processed sample of (a) copper and (b) iron-chromium alloy at position between 0 and 0.5 D/D_0 . Inhomogeneity factor of four passes ECAP is lower than one pass.

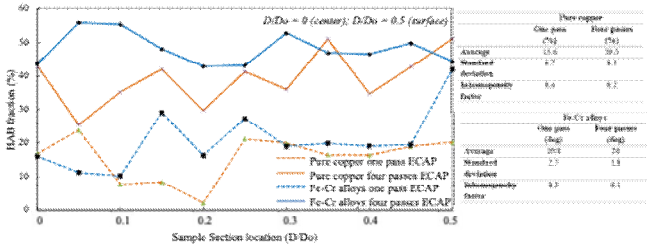

Figure 5. Mean orientation on first and fourth ECAP processed sample of (a) copper and (b) iron-chromium alloy at position between 0 and 0.5 D/D_0. Mean orientation at the sub surface showed the highest value.

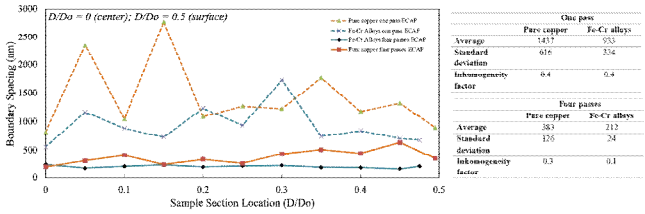

One pass

	Pure copper	Fe-Cr alloys
Average	1417	933
Standard deviation	616	334
Inhomogeneity factor	0.4	0.4

Four passes

	Pure copper	Fe-Cr alloys
Average	383	212
Standard deviation	126	24
Inhomogeneity factor	0.3	0.1

Figure 6. Boundary spacing6 on first and fourth ECAP processed sample of (a) copper and (b) iron-chromium alloy at position between 0 and 0.5 D/D_0.

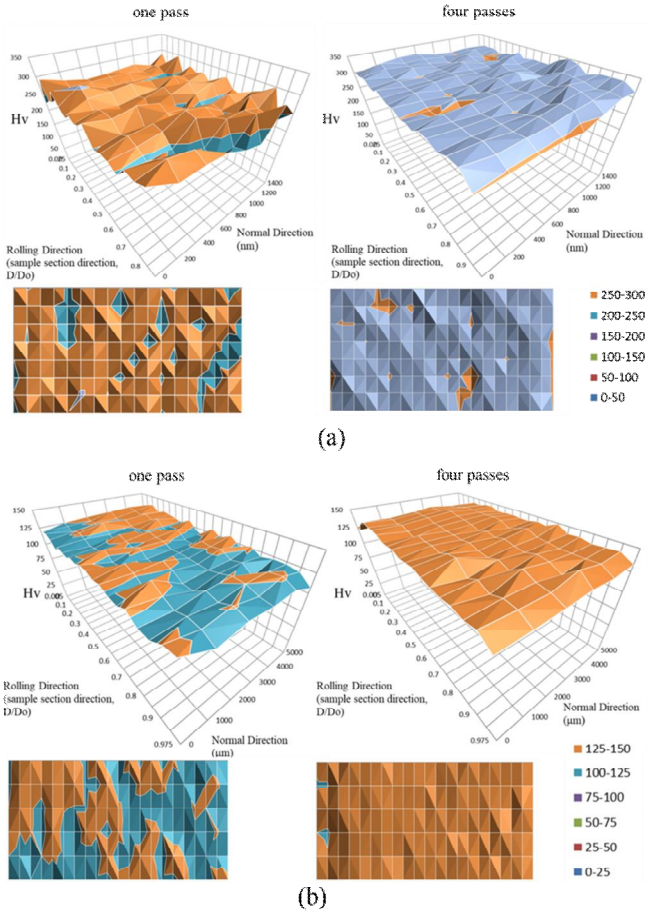

Figure 7. Hardness distribution on first and fourth ECAP processed sample in the 3D planes of (a) copper and (b) iron-chromium alloy.

The stacking fault energy directly affects the materials' recovery and recrystallization process. The boundary spacing of the ECAP processed sample can be seen in Figure 6. The boundary spacing was measured for calculating the elongated grain size due to grain shape and size. The boundary spacing on elongated grain was defined and measured by line interception drawn in the EBSD pattern image. This observation exhibited the lamellar boundary along the normal direction. The EBSD analysis only considered grain misorientation above 2° due to high error measurement below 2°, so the grain boundary measurement was carried out at misorientation higher than 2°. The D/Do = 0 and 0.5 refers to the middle and sub-surface position in the billet. The iron-chromium alloy showed more homogeneous grain boundary spacing than pure copper for one and four ECAP passes. However, the structure was more uniform after higher deformation, especially in iron-chromium alloy. The grain boundary spacing showed smaller in the middle of the billet, corresponding to the equiaxed grain after four ECAP passes at both materials. The equiaxed grain can be achieved after four passes due to the redundant process at ECAP, which can promote the high strain energy on the sample. The grain boundary spacing result concluded that the grain boundary distribution in the normalization position was uniform at four passes of ECAP.

Microhardness distribution was confirmed by Vickers hardness measurement at normalized position of ECAP billet sample. The 3D result can be revealed by the Vickers hardness result, as seen in Figure 7. It showed that the hardness distribution after four passes in iron-chromium achieved the most homogeneous among other samples due to stacking fault energy, recrystallization, and dislocation annihilation [12]. The more homogeneous structure was related to excellent grain refinement that occurred in the sample. The 3D hardness distribution result was measured by 8 points along the normal direction and 20 points along the rolling direction, with 120 points of Vickers hardness indentations. The hardness increased significantly after the first pass in both materials. However, the inhomogeneity factor was quite extensive due to the inhomogeneous structure in the transverse plane. The hardness value was scattered in the vertical axis due to initial deformation in both materials; however, the transverse axis values were constant. After four passes, the structure became uniform, and the inhomogeneity factor was smaller than the first pass. The hardness measurement in 3D was represented in color variation; therefore, it explained the hardness distribution and inhomogeneity factor clearly. The hardness distribution was measured along with the rolling and normal indicating that deformation near the subsurface was achieved during the ECAP process. The back-pressure happened during the ECAP process due to the die channel, and it increased with number of ECAP passes leading to homogeneous hardness and structure.

Figure 8 shows the TEM observation on pure copper (Figure 8.a) and iron-chromium alloy (Figure 8.b) with high dislocation density after four ECAP passes and grain refinement until 212 nm for pure copper and 257 nm for iron-chromium alloy. The TEM observation was carried out in the middle of the billet, representing the representative of ECAP sample structure. The inhomogeneity factor value was calculated in terms of boundary spacing and aspect ratio from the center until the sub-surface of the billet. This observation showed dislocation cell and sub-grain structure along the rolling plane after four ECAP passes.

The present result exhibited the lowest inhomogeneity factor due to grain refinement. The inhomogeneity factor was used in this study because this factor was accurate in comparing the SPD processes on pure copper and considered the error deviation from the hardness measurement result. Both materials also showed lower inhomogeneity factors due to homogeneous imposed strain and structure, reported in the previous work [13-16], like pure copper and stainless steel. Stacking fault energy also attributes to this behavior because of the homologous temperature process, which affects the materials' recovery and recrystallization behavior. By changing the structure of materials, it may affect to the stacking fault energy, and continuous dynamic recrystallization mechanisms occurred [9-12].

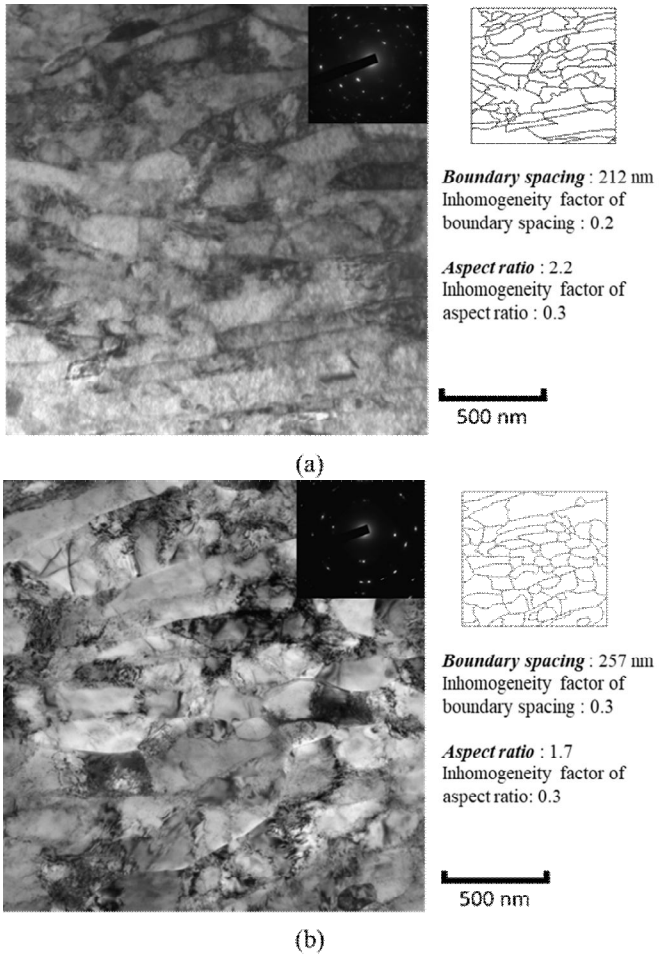

Figure 8. TEM micrograph on first and fourth ECAP processed sample of (a) copper and (b) iron-chromium alloy.

4. RESULT

The ECAP process was carried out by inserting a billet into the die channel with a sharp angle. This die channel promoted a tremendous shear strain from the middle to the subsurface, whereas the redundant process resulted in a homogeneous microstructure and mechanical properties, especially hardness. Inhomogeneity factor can be evaluated in terms of strain energy and grain refinement. This study investigated the microstructure and hardness homogeneity, which was distributed in the transverse plane with heavy deformation by ECAP. The microstructure of the ECAP process was uniform after several ECAP processes. The shear strain distribution along the transverse plane during the ECAP process was associated with microstructure evolution due to dislocation annihilation, recovery, and recrystallization [30-34]. The inhomogeneity factor was calculated by considering the standard deviation and average of the value including boundary spacing, aspect ratio, and hardness on the grain size and normal and rolling directions. The inhomogeneity factor of the boundary spacing and aspect ratio became smaller in the fourth pass than the first pass of ECAP, meaning the grain becomes an equiaxed structure at four passes of ECAP [33,34]. However, the first passes of the ECAP process showed an elongated grain structure due to a higher value of inhomogeneity. The result concluded that the grain refinement and shear strain rapidly promoted the UFG structure and homogeneous hardness due to high equivalent strain at the ECAP process.

The HAGB fraction of pure copper was smaller than that of the iron-chromium ally due to the recovery and recrystallization process during the ECAP process [30-34]. The microstructure showed the larger lamellar structure and coarser grain in the first-pass compared to the fourth pass of ECAP. The lamellar structure and partly recrystallized grain appeared along the middle of the billet by misorientation grain boundary appearance in iron-chromium alloy [35-39]. New grains were introduced at the beginning of the ECAP process associated with accumulated strain energy, recovery, and recrystallization on pure copper and iron-chromium alloy due to large deformation on the billet. The EBSD analysis revealed the recrystallized grain by showing the LAGB on the micrograph, promoting the UFG structure.

The accumulated energy strain and partial recrystallization affected HAGB formation in the first pass of ECAP on both materials [30,35]. The structure in the sub-surface was more equiaxed grain than in the middle of the billet since the plastic deformation imposed in the sub-surface was more prominent than before. This sequence promoted the fraction of HAGB significantly due to the high recovery driving force in the sub-surface [40-42]. The sub-surface exhibited a more prominent and equiaxed grain due to the warm deformation process during ECAP, related to the materials' recovery process and strain rate. The recovery process was quite difficult to appear in the iron-chromium alloy compared to pure copper due to stacking fault energy and alloying element, with lamellar structure appeared in Fe-Cr alloy smaller than that in pure copper [43]. It was concluded that the hardness inhomogeneity could be achieved during the ECAP process and could reproduce adequately.

5. CONCLUSION

The hardness increased significantly after the first pass by the ECAP process, especially in the sub-surface region due to the homologous temperature process on both materials. The hardness distribution was uniform and homogeneous due to recovery and recrystallization during the ECAP process. Lamellar boundary structure, more equiaxed grain, and the homogeneous microstructure were achieved after four passes of the ECAP process. In addition, the mean grain boundary spacing decreased by increasing the ECAP process. The pure copper and iron-chromium alloy have a different crystal structure and slip plane, affecting the material's recovery and recrystallization behavior. The hardness distribution may relate to the stacking fault energy of the material due to the high-temperature process and annihilation of dislocation. Both materials also showed lower inhomogeneity factors due to homogeneous imposed strain and structure. Stacking fault energy also attributed to this behavior because of the homologous temperature process, affecting the materials' recovery and recrystallization behavior.

REFERENCES

[1] A. Vinogradov, and Y. Estrin. **Analytical and numerical approaches to modelling severe plastic deformation**, *Progress in Materials Science*, vol. 95, pp. 172-242, 2018.

[2] Y. Cao, S. Ni, X. Liao, M. Song, and Y. Zhu. **Structural evolutions of metallic materials processed by severe plastic deformation**, *Materials Science and Engineering: R: Reports*, vol. 133, pp. 1-59, 2018.

[3] V. Segal. **Modes and processes of severe plastic deformation (SPD),** Materials, Vol. 11(7), pp. 1175, 2018.

[4] L. S. Toth, and C. Gu. **Ultrafine-grain metals by severe plastic deformation**, *Materials Characterization*, vol. 92, pp. 1-14, 2014.

[5] E. Bagherpour, N. Pardis, M. Reihanian, and R. Ebrahimi. **An overview on severe plastic deformation: research status, techniques classification, microstructure evolution, and applications**, *The International Journal of Advanced Manufacturing Technology*, vol. 100(5-8), pp. 1647-1694, 2019.

[6] S. Frint, M.Hockauf, P. Frint, and M. F. X.Wagner. **Scaling up Segal's principle of equal-channel angular pressing**, *Materials & Design*, vol. 97, pp. 502-511, 2016.

[7] R. A. Parshikov, A. I. Rudskoy, A. M. Zolotov, and O. V. Tolochko. **Technological problems of equal channel angular pressing**, *Rev. Adv. Mater. Sci*, vol. 34, pp. 26-36, 2013.

[8] K. O. Sanusi, O. D. Makinde, and G. J. Oliver. **Equal channel angular pressing technique for the formation of ultra-fine grained structures**, *South African Journal of Science*, vol. 108(9), pp. 1-7, 2012.

[9] F. Salimyanfard, M. R. Toroghinejad, F. Ashrafizadeh, M. Hoseini, and J. A. Szpunar. **Investigation of texture and mechanical properties of copper processed by new route of equal channel angular pressing**, *Materials & Design*, vol. 44, pp. 374-381, 2013.

[10] G. G. Maier, E. G. Astafurova, H. J. Maier, E. V. Naydenkin, G. I. Raab, P. D. Odessky, and S.V. Dobatkin. **Annealing behavior of ultrafine grained structure in low-carbon steel produced by equal channel angular pressing**, *Materials Science and Engineering: A*, vol. 581, pp. 104-107, 2013.

[11] S. Lezhnev, I. Volokitina, and T. Koinov. **Research of Influence Equal Channel Angular Pressing on The Microstructure of Copper**, *Journal of Chemical Technology & Metallurgy*, vol. 49(6), pp. 1, 2014.

[12] H. Miyamoto, M. Yuasa, M. Rifai, and H. Fujiwara. **Corrosion behavior of severely deformed pure and single-phase materials**, *Materials Transactions*, vol. 60(7), pp. 1243-1255, 2019.

[13] M. Rifai, H. Miyamoto, and H. Fujiwara. **Effects of strain energy and grain size on corrosion resistance of ultrafine grained Fe-20% Cr steels with extremely low C and N fabricated by ECAP**, *International Journal of Corrosion*, vol. 2015, 2015.

[14] M. Rifai, M. Yuasa, and H. Miyamoto. **Enhanced corrosion resistance of ultrafine-grained Fe-Cr alloys with subcritical Cr contents for passivity**, *Metals*, vol. 8(3), pp. 149, 2018.

[15] M. Rifai, and H. Miyamoto. **Effect of stored energy on corrosion fatigue properties of ultrafine grained Fe-20% Cr steel by equal channel angular pressing**, *IOP Conference Series: Materials Science and Engineering*, Vol. 673, pp. 012131, 2019.

[16] M. Rifai, M. Yuasa, and H. Miyamoto. **Effect of Deformation Structure and Annealing Temperature on Corrosion of Ultrafine-Grain Fe-Cr Alloy Prepared by Equal Channel Angular Pressing**, *International Journal of Corrosion*, vol. 2018, 2018.

[17] M. Y. Alawadhi, S. Sabbaghianrad, Y. Huang, and T. G. Langdon. **Direct influence of recovery behaviour on mechanical properties in oxygen-free copper processed using different SPD techniques: HPT and ECAP**, *Journal of Materials Research and Technology*, vol. 6(4), pp. 369-377, 2017.

[18] A. P. Zhilyaev, and T. G. Langdon. **Microhardness and EBSD microstructure mapping in partially-pressed al and cu through 90º ECAP die**, *Materials Research*, vol. 16, pp. 586-591, 2013.

[19] M. Y. Alawadhi, S. Sabbaghianrad, Y. Huang, and T. G. Langdon. **Evaluating the paradox of strength and ductility in ultrafine-grained oxygen-free copper processed by ECAP at room temperature**, *Materials Science and Engineering: A*, vol. 802, pp. 140546, 2021.

[20] M. Zhang, L. Liu, S. Liang, and J. Li. **Evolution in microstructures and mechanical properties of pure copper subjected to severe plastic deformation**, *Metals and Materials International*, vol. 26(10), pp.1585-1595, 2020.

[21] L. Zhang, A. Ma, J. Jiang, and X. Jie. **Effect of processing methods on microhardness and acid corrosion behavior of low-carbon steel**, *Materials & Design*, vol. 65, pp. 115-119, 2015.

[22] Z. J. Zheng, J. W. Liu, and Y. Gao. **Achieving high strength and high ductility in 304 stainless steel through bi-modal microstructure prepared by post-ECAP annealing**, *Materials Science and Engineering: A*, vol. 680, pp. 426-432, 2017.

[23] A. M. Kliauga, V. L. Sordi, and S. V. Dobatkin. **Microstructural evolution of a F138 austenitic stainless steel after deformation by ECAP and HPT**, *Materials Science Forum*, vol. 775, pp. 482-486, 2014.

[24] M. Toofaninejad, and M. N. Ahmadabadi. **Effect of equal channel angular pressing on the microstructure and mechanical properties of AISI type 304 austenitic stainless steel**, *Advanced Materials Research* (Vol. 829, pp. 86-90). Trans Tech Publications Ltd. (2014)

[25] A. V. Filippov, S. Y. Tarasov, S. V. Fortuna, O. A. Podgornykh, N. N. Shamarin, and V. E. Rubtsov. **Microstructural, mechanical and acoustic emission-assisted wear characterization of equal channel angular pressed (ECAP) low stacking fault energy brass**, *Tribology International*, vol. 123, pp. 273-285, 2018.

[26] A. I. Alateyah, M. M. Ahmed, Y. Zedan, H. A. El-Hafez, M. O. Alawad, and W. H. El-Garaihy. **Experimental and Numerical Investigation of the ECAP Processed Copper: Microstructural Evolution, Crystallographic Texture and Hardness Homogeneity**, *Metals*, vol. 11(4), pp. 607, 2021.

[27] J. Wongsa-Ngam, M. Kawasaki, and T. G. Langdon. **The development of hardness homogeneity in a Cu–Zr alloy processed by equal-channel angular pressing**, *Materials Science and Engineering: A*, vol. 556, pp. 526-532, 2012.

[28] M. Ma, Z. Li, W. Qiu, Z. Xiao, Z. Zhao, Y. Jiang, and H. Huang. **Development of homogeneity in a Cu-Mg-Ca alloy processed by equal channel angular pressing**, *Journal of Alloys and Compounds*, vol. 820, pp. 153112, 2020.

[29] F. Djavanroodi, M. Daneshtalab, and M. Ebrahimi. **A novel technique to increase strain distribution homogeneity for ECAPed materials**, *Materials Science and Engineering: A*, vol. 535, pp. 115-121, 2012.

[30] O. Šedivý, V. Beneš, P. Ponížil, P.Král, and V. Sklenička. **Quantitative characterization of microstructure of pure copper processed by ECAP**, *Image Analysis and Stereology*. (2013)

[31] N. D. Stepanov, A. V. Kuznetsov, G. A. Salishchev, G. I. Raab, and R. Z. Valiev. **Effect of cold rolling on microstructure and mechanical properties of copper subjected to ECAP with various numbers of passes**, *Materials Science and Engineering: A*, vol. 554, pp. 105-115, 2012.

[32] J. Bach, J. P. Liebig, H. W. Höppel, and W.Blum. **Influence of grain boundaries on the deformation resistance: insights from an investigation of deformation kinetics and microstructure of copper after predeformation by ECAP**, *Philosophical Magazine*, vol. 93(35), pp. 4331-4354, 2013.

[33] K. Hirayama, K. Nagai, H. Fujiwara, and H. Miyamoto. **Effect of grain boundary structure on misorientation change of pure copper bicrystals pressed by one-pass equal-channel angular pressing**, *Materials Transactions*, vol. 54(7), pp. 1077-1082, 2013.

[34] W. Feng, J. H. Zhang, and S. Yang. **Grain Boundary Engineering of ECAPed OFHC Copper**, Materials Science Forum, vol. 879, pp. 2192-2197, 2017.

[35] K. Hajizadeh, H. Maleki-Ghaleh, A. Arabi, Y. Behnamian, E. Aghaie, A. Farrokhi, and M. H. Fathi. **Corrosion and biological behavior of nanostructured 316L stainless steel processed by severe plastic deformation**, *Surface and Interface Analysis*, vol. 47(10), 978-985. (2015)

[36] L. Jinlong, and W. Zhuqing. **Deformed nanotwins promoted by grain refinement in austenitic stainless steel and its characteristics**, *Materials Letters*, vol. 282, pp.128708, 2021.

[37] N. S. De Vincentis, A. Kliauga, M. Ferrante, M. Avalos, H. G. Brokmeier, and R. E. Bolmaro. **Evaluation of microstructure anisotropy on room and medium temperature ECAP deformed F138 steel**, *Materials Characterization*, vol. 107, pp. 98-111, 2015.

[38] Z. J. Zheng, Y. Gao, J. W. Liu, and M. Zhu. **A hybrid refining mechanism of microstructure of 304 stainless steel subjected to ECAP at 500 C**, *Materials Science and Engineering: A*, vol. 639, pp. 615-625, 2015.

[39] M. Eddahbi, R. Domínguez-Reyes, M. A. Monge, A. Muñoz, and R.Pareja. **Grain boundary misorientation and positron annihilation characteristics in steel Eurofer processed by equal channel angular pressing**, *Journal of Materials Science*, vol. 49(19), pp. 6722-6733, 2014.

[40] C. X. Huang, W. Hu, G. Yang, Z. F. Zhang, S. D. Wu, Q. Y. Wang, and G. Gottstein. **The effect of stacking fault energy on equilibrium grain size and tensile properties of nanostructured copper and copper–aluminum alloys processed by equal channel angular pressing**, *Materials Science and Engineering: A*, vol. 556, pp. 638-647, 2012.

[41] S. E. Mousavi, A. Sonboli, N. Naghshehkesh, M. Meratian, A. Salehi, and M. Sanayei. **Different behavior of alpha and beta phases in a Low Stacking Fault Energy copper alloy under severe plastic**

deformation, *Materials Science and Engineering: A*, vol. 788, pp. 139550, 2020

[42] F. Liu, Y. Huan, J. Yin, and J. T. Wang. **Influence of stacking fault energy and temperature on microstructures and mechanical properties of fcc pure metals processed by equal-channel angular pressing**, *Materials Science and Engineering: A*, vol. 662, pp. 578-587, 2016.

[43] M. Zohrevand, M. Aghaie-Khafri, F. Forouzan, and E.Vuorinen. **Microstructural evolutions under ultrasonic treatment in 304 and 316 austenitic stainless steels: impact of stacking fault energy**, *Steel Research International*, vol. 2100041, pp. 1, 2021.

[44] M. Dani, S. Mustofa, S. Parikin, T. Sudiro, B. Hermanto, D. R. Adhika, A. Insani, A. Dimyati, S. H. Syahbuddin, E. A. Basuki, and C. A. Huang. **Effect of Spark Plasma Sintering (SPS) at Temperatures of 900and 950 o c for 5 Minutes on Microstructural Formation of Fe-25Ni-17Cr Austenitic Stainless Steel**, *International Journal of Emerging Trends in Engineering Research*, vol. 8, no. 8, 2020.